

Supplemental Information

Circulating Triglycerides Gate Dopamine-Associated

Behaviors through DRD2-Expressing Neurons

Chloé Berland, Enrica Montalban, Elodie Perrin, Mathieu Di Miceli, Yuko Nakamura, Maud Martinat, Mary Sullivan, Xue S. Davis, Mohammad Ali Shenasa, Claire Martin, Stefania Tolu, Fabio Marti, Stephanie Caille, Julien Castel, Sylvie Perez, Casper Gravesen Salinas, Chloé Morel, Jacob Hecksher-Sørensen, Martine Cador, Xavier Fioramonti, Matthias H. Tschöp, Sophie Layé, Laurent Venance, Philippe Faure, Thomas S. Hnasko, Dana M. Small, Giuseppe Gangarossa, and Serge H. Luquet

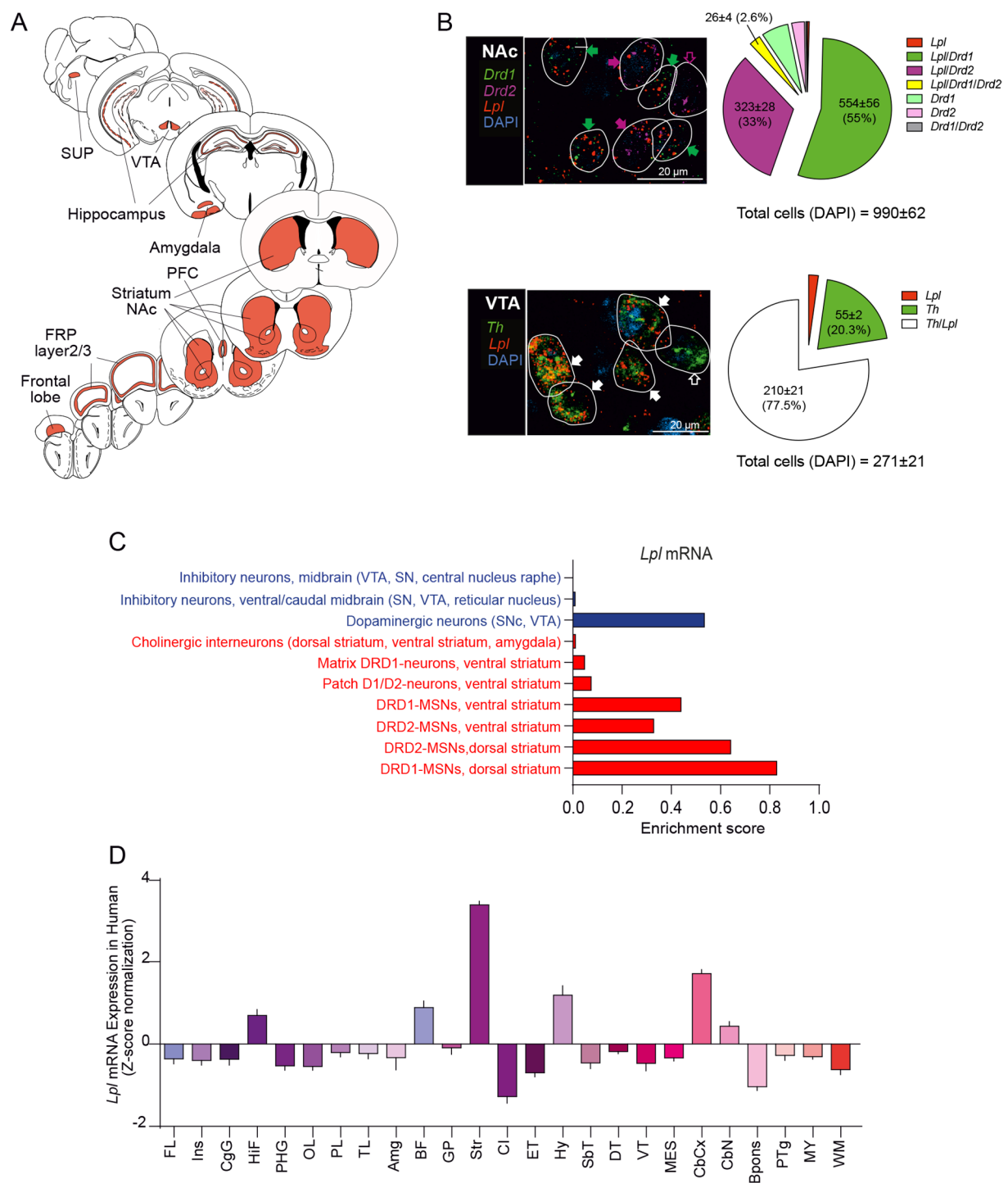


Figure S1. Distribution of *Lpl* mRNA in the mesocorticolimbic system. Related to Figure 1. (A) Central *in situ* hybridization detection of *Lpl* mRNA in C57Bl6/J mouse brain (male) from the Allen Institute. FRP: frontal pole layer, NAc: nucleus accumbens, PFC: prefrontal cortex, VTA: ventral tegmental area, SUP: pontine structures. **(B)** Representative photomicrographs and semi-quantitative analysis of RNAscope fluorescence *in situ* hybridization (FISH) signal for Lipoprotein lipase (*Lpl*, red), tyrosine hydroxylase (*Th*, green), dopamine receptor 1 and 2

(*Drd1* green, *Drd2* violet) in the ventral tegmental area (VTA) and the nucleus accumbens (NAc). DAPI (blue) was used to identify cells. Scale bars: 20 μ m. The white lines represent the cellular limits. Filled and empty arrows within representative photomicrographs indicate co-expression or absence, respectively, of *Lpl* according to the presence of *Th* (white arrows), *Drd1* (green arrows) and *Drd2* (violet arrows) transcripts. **(C)** *Lpl* mRNA enrichment score in different midbrain (blue) and striatal (red) cells extracted from single-cell RNA sequencing atlas (Zeisel et al., 2018) (<http://mousebrain.org/genesearch.html>). Data are plotted as function of the enrichment score and filtered by trinarization score >0.95. **(D)** Quantification of *Lpl* expression in human brain structures based on the Allen Institute database. Structures: FL (frontal lobe), Ins (insula), CgG (cingulate gyrus), HiF (hippocampal formation), PHG (parahippocampal gyrus), OL (occipital lobe), PL (parietal lobe), TL (temporal lobe), Amg (amygdala), BF (basal forebrain), GP (globus pallidus), Str (striatum), CI (claustrum), ET (epithalamus), Hy (hypothalamus), Sbt (subthalamus), DT (dorsal thalamus), VT (ventral thalamus), MES (mesencephalon), CbCx (cerebellar cortex), CbN (cerebellar nuclei), Bpons (basal part of pons), PTg (pontine tegmentum), MY (myelencephalon), WM (white matter).

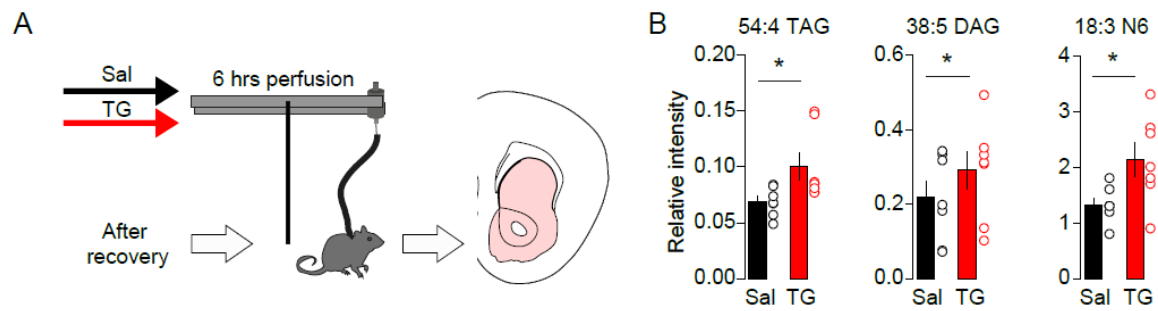


Figure S2. Lipidomic analysis following central TG delivery. Related to Figure 1.

(A) Experimental design of brain TG delivery technique. Animals were perfused through the carotid for 6-hours (6-hrs) with saline (Sal) or Intralipid™ (TG). Striata were dissected and used for lipidomic analysis. **(B)** Lipidomic analysis of 54:4 TAG, 38:5 DAG and 18:3 N6 FFA contents in the striatum of animals centrally perfused with saline (Sal, n=7) or TG (TG, n=7). Statistics: * $p < 0.05$ Sal vs TG. For statistical details see Table S5.

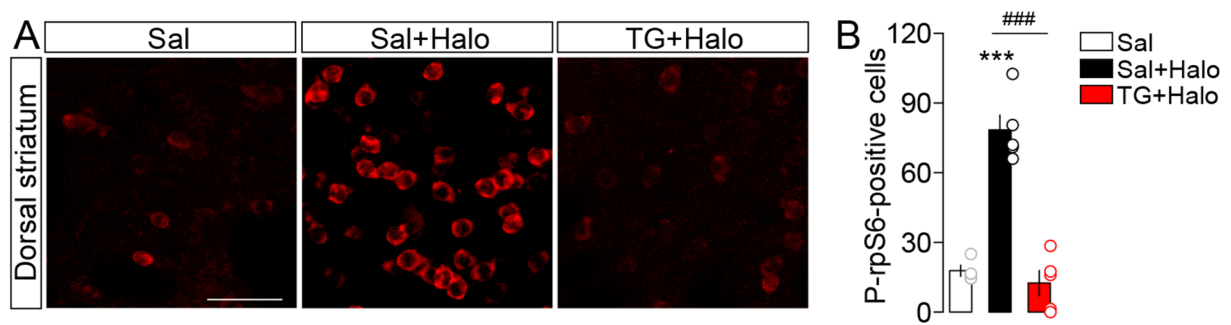
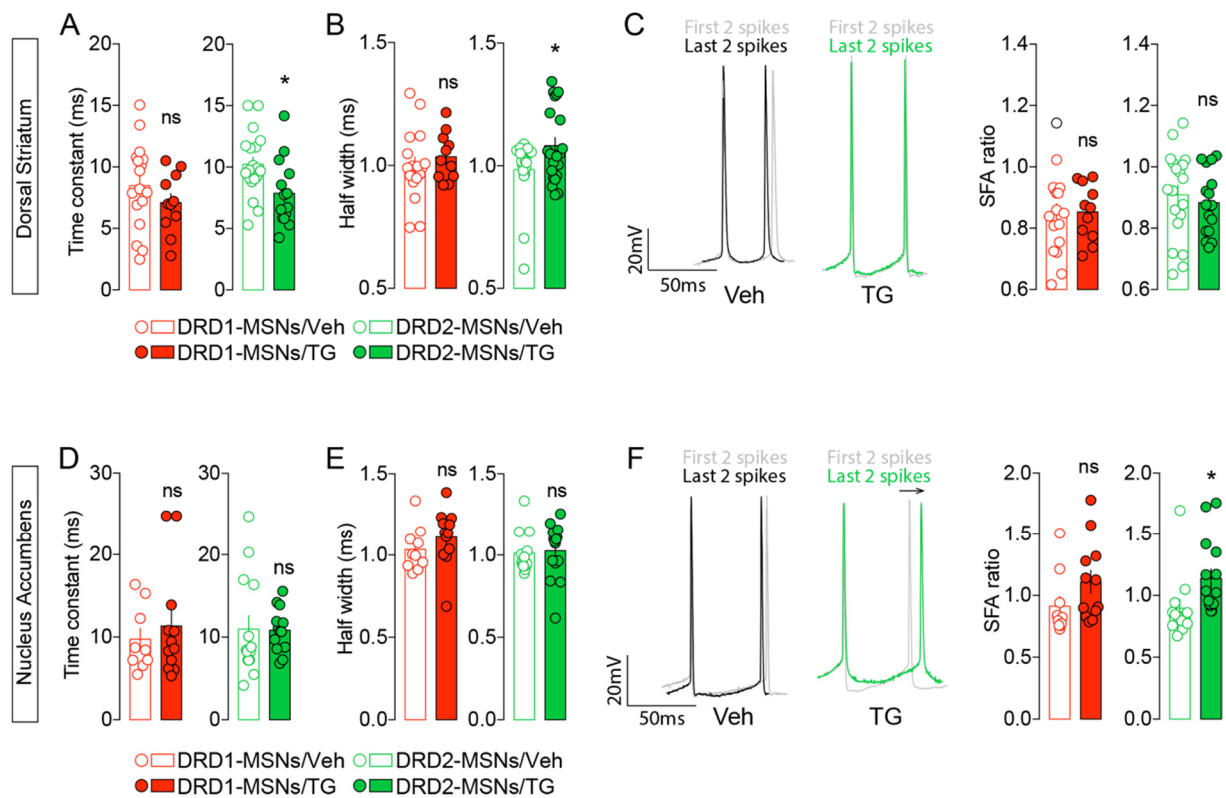


Figure S3. Central TG delivery blunts DRD2-dependent striatal signaling pathways. Related to Figure 2.

(A) Representative confocal photomicrographs and (B) quantification of phosphor-rpS6^{Ser235/236}-positive cells in the dorsal striatum of animals infused with saline and injected with saline (Sal, n=4) or haloperidol (Sal/Halo, n=5) and animals infused with TG and injected with haloperidol (TG/Halo, n=5). Scale bar: 50 μ m. Statistics (multiple comparisons): (***)p<0.001 Sal+Halo vs Sal; (###)p<0.001 TG+Halo vs Sal+Halo). For statistical details see Table S5.



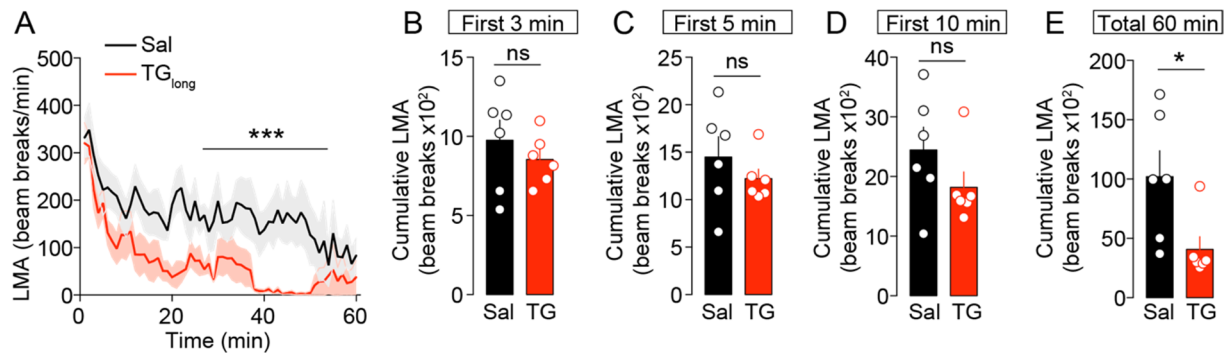


Figure S5. Effect of central TG delivery on novelty-induced locomotor activity. Related to Figure 3.

(A) Time course analysis of the locomotor activity (LMA) during the exploratory phase of a novel environment (new cage) following 6-hrs infusion of saline or TG. Cumulative analysis of exploratory activity following 3 (B), 5 (C), 10 (D) and 60 (E) minutes. Statistics (single or multiple comparisons): A (2-Way ANOVA: treatment effect ***p<0.001), E (*p<0.05 TG vs Sal). For statistical details see Table S5.

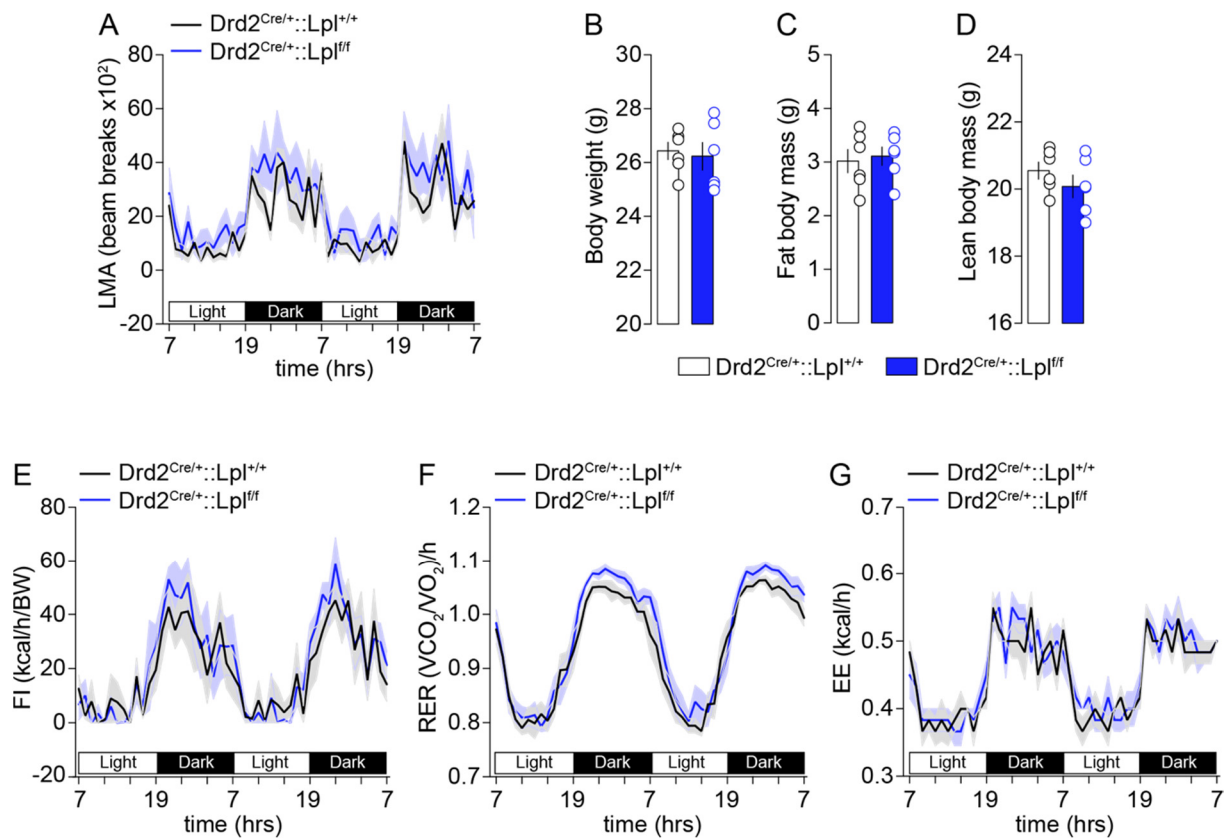


Figure S6. Intact basal metabolism following genetic deletion of Lpl in DRD2-expressing cells. Related to Figure 6.

(A) Locomotor activity in control ($\text{Drd2}^{\text{Cre/+}}::\text{Lpl}^{+/+}$) and cKO ($\text{Drd2}^{\text{Cre/+}}::\text{Lpl}^{\text{fl/f}}$) mice during two consecutive days. Histograms indicate body weight (B), fat body mass (C) and lean body mass (D). Food intake (FI, E), respiratory exchange ratio (RER, F) and energy expenditure (EE, G) in control ($\text{Drd2}^{\text{Cre/+}}::\text{Lpl}^{+/+}$) and cKO ($\text{Drd2}^{\text{Cre/+}}::\text{Lpl}^{\text{fl/f}}$) mice during two consecutive days. No differences were observed between experimental groups. For statistical details see Table S5.

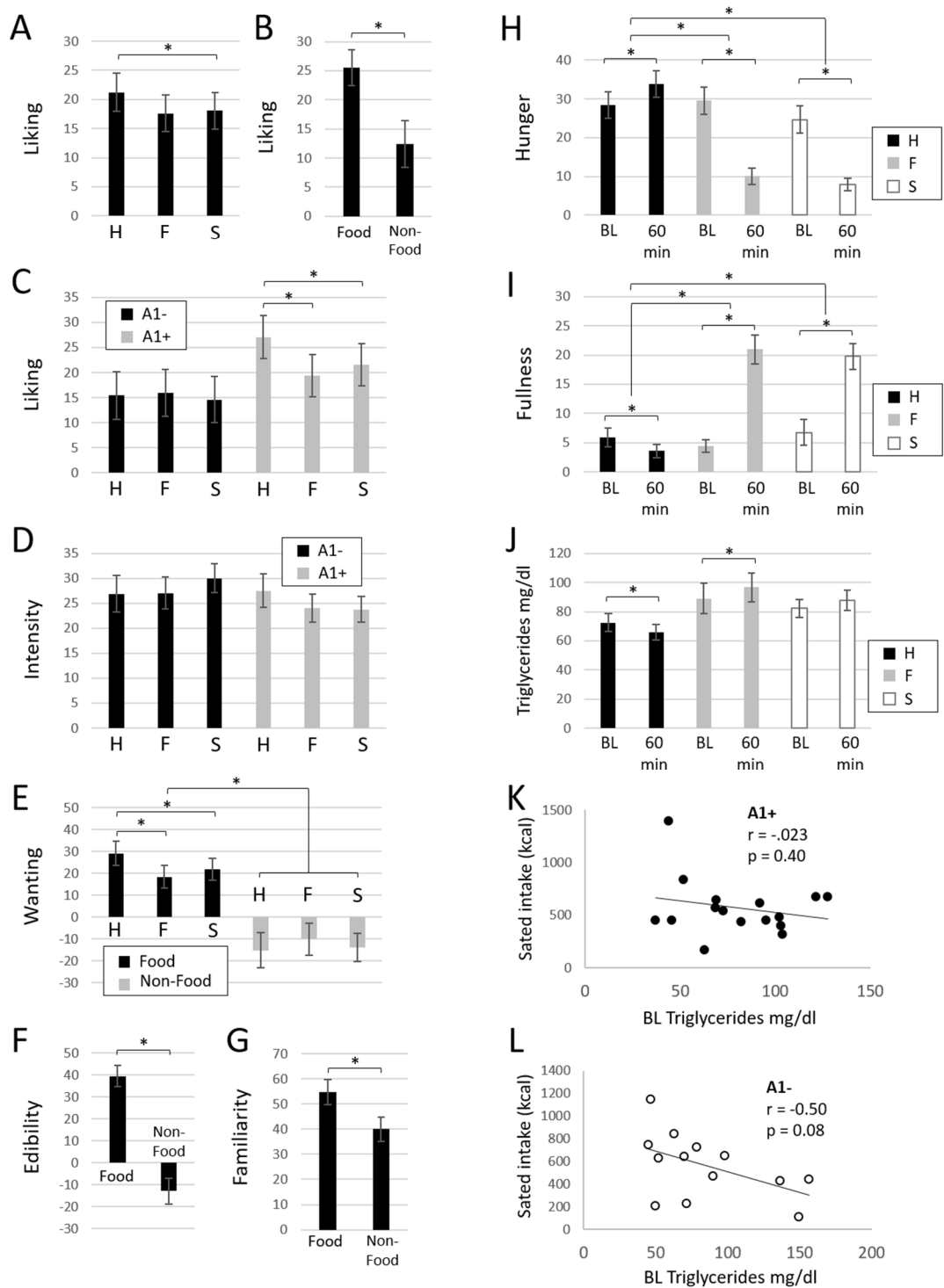


Figure S7. Metabolic and internal state ratings in humans. Related to Figure 7.

(A-C) Ratings of odor liking. There were significant effects of condition (A; $F_{(2,54)}=3.78$, $p=0.029$) and odor (B; $F_{(1,27)}=13.18$, $p=0.001$) as well as an interaction between condition and group (C; $F_{(2,54)}=4.17$, $p=0.031$). *Post hoc* tests revealed that liking ratings in Hungry condition

were greater than that in Sated condition ($p=0.026$), and liking ratings for food odor were greater than ratings for non-food odor ($p=0.001$). In the A1+ but not A1- group, liking ratings for all odors were greater in the Hungry condition than in Fixed ($p=0.003$) or Sated ($p=0.005$) conditions. **(D)** Ratings of odor intensity. There was a significant interaction between condition and group ($F_{(2,54)}=3.21$, $p=0.048$). However, post-hoc tests revealed no statistically significant pairwise comparisons. **(E)** Ratings of odor wanting. There was a significant effect of odor ($F_{(1,27)}=35.72$, $p<0.001$) as well as a condition by odor interaction ($F_{(2,54)}=3.17$, $p=0.05$). Post-hoc tests showed that wanting ratings for food odor were greater than that for non-food odor ($p<0.001$), and that for food but not non-food odors, wanting ratings were greater under the Hungry condition than under Fixed ($p=0.036$) or Sated ($p=0.049$) conditions. **(F)** Ratings of odor edibility. There was a significant effect of odor ($F_{(1,27)}=47.86$, $p<0.001$) where edibility ratings for food odors were greater than those for non-food odors. **(G)** Ratings of odor familiarity. There was significant effect of odor on ratings for familiarity ($F_{(1,27)}=23.32$, $p<0.001$) where familiarity ratings for food odors were greater than those for non-food odors ($p<0.001$). **(H)** Ratings of hunger. There were significant effects of condition ($F_{(2,54)}=50.33$, $p<0.001$) and time ($F_{(1,27)}=26.03$, $p<0.001$), as well as an interaction between condition and time ($F_{(2,54)}=33.05$, $p<0.001$). Hunger ratings increased from baseline to 60 min in the Hungry condition ($p=0.031$), but decreased over the same time span in the Fixed ($p<0.001$) and Sated ($p<0.001$) conditions. **(I)** Ratings of fullness. There were significant effects of condition ($F_{(2,54)}=36.13$, $p<0.001$), time ($F_{(1,27)}=62.70$, $p<0.001$), as well as an interaction between condition and time ($F_{(2,54)}=36.15$, $p<0.001$). Fullness ratings decreased from baseline to 60 min in the Hungry condition ($p=0.004$), but increased over the same time span in the Fixed ($p<0.001$) and Sated ($p<0.001$) conditions. **(J)** Circulating plasma triglyceride levels. There was a significant effect of condition ($F_{(2,54)}=8.00$, $p=0.001$) as well as a condition by time interaction ($F_{(2,54)}=10.15$, $p<0.001$). Triglyceride levels decreased from baseline to 60 min in the Hungry condition ($p<0.001$) and increased over the same time span in the Fixed condition ($p=0.010$). There was a trend towards an increase in triglycerides from baseline to 60 min in the Sated condition ($p=0.055$). **(K)** TG level correlations with caloric intake in sated participants as a function of genotype. No relationship was observed in A1+ while a trend **(L)** was evident in A1-. This is despite the fact that there was no significant difference in intake calories from lunch in the Sated condition between groups ($p=0.91$). Nevertheless, we elected to focus imaging analyses on the Fixed scan where intake is held constant. H = Hungry condition, F = Fixed condition, S = Sated condition; BL = baseline; 60 min = 60 min after meal or baseline. Error bars represent standard error of the mean. For statistical details see Table S5.

Supplementary Tables

Glycerolipid	SAL (relative intensity/mg protein)	TG (relative intensity/mg protein)	p-value
54:4 TAG	0.06899	0.1007	0.0141
60:9 TAG	0.005516	0.008994	0.0189
52:4 TAG	0.0579	0.08414	0.0202
54:5 TAG	0.05881	0.07751	0.0287
38:5 DAG	0.2182	0.2913	0.0332
50:2 TAG	0.1099	0.1594	0.0332
56:6 TAG	0.162	0.2352	0.0379
50:0 TAG	0.3527	0.4922	0.04
56:4 TAG	0.0229	0.03254	0.0459
52:3 TAG	0.1152	0.1581	0.048
60:12 TAG	0.05009	0.08068	0.0481
50:3 TAG	0.01548	0.01944	0.0494
56:5 TAG	0.05221	0.06834	0.0533
52:2 TAG	0.3677	0.4823	0.0536
Total TAG	3.528	4.655	0.0649
54:1 TAG	0.07028	0.08915	0.068
50:1 TAG	0.4231	0.6237	0.0843
60:11 TAG	0.01862	0.02401	0.092
58:6 TAG	0.01411	0.01989	0.0938
48:1 TAG	0.06114	0.07601	0.0998

Free Fatty Acid	SAL (relative intensity/mg protein)	TG (relative intensity/mg protein)	p-value
18:3 N6	1.329	2.143	0.0216
20:3 N9	1.071	1.629	0.0554

Table S1. Intracarotid TG delivery leads to change in striatal fatty acids and glycolipids content. Related to Figure 1 and S1. Lipidomics analysis of significant TAG, DAG and FFA changes found in the striata of mice perfused with TG or saline. Raw data for fatty acids and glycolipids are provide in Data S1 & S2

	Dorsal striatum (DS)			
	DRD1-MSNs		DRD2-MSNs	
	Veh (n=15-17)	TG (n=10-11)	Veh (n=18-19)	TG (n=14-21)
RMP (mV)	-75.24 ± 1.43	-76.18 ± 1.27	-73.93 ± 0.77	-81.05 ± 0.63 ***
Rheobase (pA)	150.3 ± 15.64	173.5 ± 21.25	99.17 ± 8.59	124.5 ± 15.69
Resistance (Mohm)	93.49 ± 7.03	102.1 ± 13.0	126.9 ± 9.03	131.1 ± 15.28
AP amplitude (mV)	88.17 ± 4.23	92.93 ± 2.79	94.66 ± 1.57	91.15 ± 2.70
Half width (ms)	0.99 ± 0.03	1.03 ± 0.03	0.98 ± 0.03	1.08 ± 0.03 *
AP threshold (mV)	-34.74 ± 1.54	-36.37 ± 1.51	-38.22 ± 0.96	-36.03 ± 1.29
fAHP amplitude (mV)	15.19 ± 1.47	17.27 ± 1.91	18.12 ± 2.01	16.70 ± 1.18
AP rise time (ms)	0.31 ± 0.02	0.34 ± 0.01	0.27 ± 0.01	0.32 ± 0.01 *
AP decay (ms)	0.92 ± 0.03	0.93 ± 0.05	0.99 ± 0.04	1.05 ± 0.03
SFA ratio	0.848 ± 0.03	0.853 ± 0.03	0.91 ± 0.03	0.88 ± 0.03
Time constant (ms)	8.48 ± 0.85	7.09 ± 0.73	10.23 ± 0.59	7.88 ± 0.72 *

	Statistics (unpaired t-test)	
	DRD1-MSNs (Veh vs TG)	DRD2-MSNs (Veh vs TG)
RMP (mV)	p=0.649, t=0.4602 df=26	*** p<0.0001, t=7.241 df=37
Rheobase (pA)	p=0.379, t=0.8971 df=23	p=0.178, t=1.373 df=36
Resistance (Mohm)	p=0.532, t=0.6338 df=26	p=0.819, t=0.231 df=36
AP amplitude (mV)	p=0.414, t=0.8294 df=26	p=0.289, t=1.076 df=37
Half width (ms)	p=0.471, t=0.7317 df=26	* p=0.039, t=2.133 df=37
AP threshold (mV)	p=0.479, t=0.7175 df=26	p=0.194, t=1.322 df=37
fAHP amplitude (mV)	p=0.391, t=0.8716 df=26	p=0.535, t=0.627 df=37
AP rise time (ms)	p=0.177, t=1.388 df=26	* p=0.021, t=2.401 df=37
AP decay (ms)	p=0.842, t=0.201 df=26	p=0.200, t=1.304 df=37
SFA ratio	p=0.915, t=0.1078 df=26	p=0.556, t=0.5911 df=33
Time constant (ms)	p=0.261, t=1.149 df=26	* p=0.017, t=2.524 df=31

Table S2. Bath application of triolein affect DRD2-MSNs activity in the dorsal striatum. Related to Figure 3 and S4. Electrophysiological parameters of DRD1- and DRD2-MSNs in the dorsal striatum (DS) following bath application of triolein.

	Nucleus Accumbens (NAc)			
	DRD1-MSNs		DRD2-MSNs	
	Veh (n=10)	TG (n=12-13)	Veh (n=13)	TG (n=15)
RMP (mV)	-72.90 ± 2.23	-75.83 ± 1.92	-71.77 ± 2.24	-76.73 ± 1.13 *
Rheobase (pA)	90.83 ± 12.02	93.08 ± 14.07	116.0 ± 22.15	103.0 ± 9.63
Resistance (Mohm)	155.6 ± 23.84	205.3 ± 41.42	178.6 ± 27.49	123.4 ± 20.02
AP amplitude (mV)	92.06 ± 1.21	85.71 ± 1.91 *	91.36 ± 1.18	80.77 ± 2.42 ***
Half width (ms)	1.03 ± 0.04	1.11 ± 0.05	1.01 ± 0.03	1.02 ± 0.04
AP threshold (mV)	-38.80 ± 1.70	-34.79 ± 1.45	-35.63 ± 1.36	-34.76 ± 1.01
fAHP amplitude (mV)	14.19 ± 0.97	13.39 ± 0.67	13.89 ± 0.78	15.58 ± 1.46
AP rise time (ms)	0.27 ± 0.02	0.32 ± 0.02	0.26 ± 0.01	0.32 ± 0.01 *
AP decay (ms)	1.14 ± 0.06	1.09 ± 0.06	1.08 ± 0.05	0.99 ± 0.05
SFA ratio	0.91 ± 0.08	1.11 ± 0.09	0.89 ± 0.07	1.14 ± 0.08 *
Time constant (ms)	9.73 ± 1.31	11.34 ± 1.94	10.97 ± 1.63	10.84 ± 0.74

	Statistics (unpaired t-test)	
	DRD1-MSNs (Veh vs TG)	DRD2-MSNs (Veh vs TG)
RMP (mV)	p=0.328, t=1,002 df=20	* p=0.049, t=2.058 df=26
Rheobase (pA)	p=0.908, t=0.1167 df=21	p=0.576, t=0.5656 df=26
Resistance (Mohm)	p=0.336, t=0.9865 df=20	p=0.111, t=1.651 df=26
AP amplitude (mV)	* p=0.014, t=2.673 df=20	*** p<0.0001, t=3.748 df=26
Half width (ms)	p=0.263, t=1.153 df=20	p=0.807, t=0.2469 df=26
AP threshold (mV)	p=0.087, t=1.8 df=20	p=0.603, t=0.5261 df=26
fAHP amplitude (mV)	p=0.498, t=0.6897 df=20	p=0.337, t=0.9784 df=26
AP rise time (ms)	p=0.077, t=1.865 df=20	* p=0.014, t=2.631 df=26
AP decay (ms)	p=0.648, t=0.4681 df=20	p=0.211, t=1.281 df=26
SFA ratio	p=0.125, t=1.558 df=20	* p=0.031, t=2.285 df=26
Time constant (ms)	p=0.529, t=0,6412 df=19	p=0.945, t=0.06918 df=25

Table S3. Bath application of triolein affect DRD2-MSNs activity in the Nucleus Accumbens. Related to Figure 3 and S4. Electrophysiological parameters of DRD1- and DRD2-MSNs in the nucleus accumbens (NAc) following bath application of triolein.

	Nucleus accumbens (NAc)	
	mCherry positive DRD2-MSNs	
	Control (n=33)	cKO (n=33)
RMP (mV)	-78.58 ± 1.32	-75.11 ± 1.50
Membrane capacitance (pF)	84.08 ± 6.20	80.23 ± 4.98
Resistance (MOhm)	191.3 ± 14.63	225.1 ± 13.53
Rectification index	0.903 ± 0.007	0.8921 ± 0.006
Rheobase (pA)	64.24 ± 7.50	55.76 ± 4.73
Delay to 1st spike (ms)	292.5 ± 21.62	233.0 ± 20.78
AP threshold (mV)	-38.28 ± 0.72	-38.10 ± 0.77
AP amplitude (mV)	64.03 ± 1.87	62.88 ± 1.36
AP duration (ms)	5.28 ± 0.30	5.33 ± 0.22
fAHP amplitude (mV)	8.23 ± 0.56	7.97 ± 0.54
AP rise (mV/ms)	41.20 ± 2.55	40.02 ± 2.03
AP decay (mV/ms)	21.35 ± 1.95	18.47 ± 0.95

	Statistics (NAc)	
	Unpaired t-test	Mann-Whitney test
RMP (mV)	p=0.088, t=1.734 df=64	
Membrane capacitance (pF)	p=0.629, t=0.4844 df=64	
Resistance (MOhm)		* p=0.047, U=390
Rectification index		p=0.124, U=424
Rheobase (pA)		p=0.703, U=514.5
Delay to 1st spike (ms)	p=0.051, t=1.986 df=64	
AP threshold (mV)	p=0.866, t=0.1695 df=64	
AP amplitude (mV)	p=0.619, t=0.4993 df=64	
AP duration (ms)		p=0.568, U=499.5
fAHP amplitude (mV)	p=0.740, t=0.3333 df=64	
AP rise (mV/ms)	p=0.719, t=0.3614 df=64	
AP decay (mV/ms)	p=0.189, t=1.327 df=64	

Table S4. *Lpl* expression regulates DRD2-MSNs excitability. Related to Figure 6.
Electrophysiological parameters of NAc DRD2-MSNs following genetic deletion of *Lpl*.